Numerical modelling of slurry transport for coarse particles

Xiong, Ting; Xinzu, Zhang; Miedema, S. A.; Xiuhan, Chen

Publication date
2019

Document Version
Final published version

Published in
Proceedings 22nd World Dredging Congress

NUMERICAL MODELLING OF SLURRY TRANSPORT FOR COARSE PARTICLES

Xiuhan Chen[1], Ting Xiong[2], Xinzuo Zhang[3], Sape A. Miedema[4]

ABSTRACT

Transportation of the coarse materials is one of the major challenges in slurry transport for dredging. Unfavorable situations may occur, e.g., the strong hydraulic resistance and the blocking in the pipe. In this study, An Eulerian-Lagrangian coupled algorithm is implemented to model the pipeline transport process of coarse particles. Codes of computational fluid dynamics (CFD) and discrete element modeling (DEM) are utilized for simulating the fluid and the solid behavior respectively. The numerical modeling of particles with a diameter of 10mm transported in a pipeline with a diameter of 15.24cm is carried out under three different conveying line speeds. Qualitative study is made on the transitions between different flow regimes, and quantitative analysis is made on the volumetric concentration and the hydraulic gradient in the pipe.

Key words: coarse particles; slurry transport; volumetric concentration; sliding bed

1. Introduction and literature review

Hydraulic transport is a transportation method that uses water as a carrier to transport solid materials [1]. It has advantages in low pollution, high energy effeciency, weather-free condition, and high capacity, hydraulic transport is widely used in many kinds of engineering practices [2]. With the continuous development in the pipeline application, the range of the sizes of the transported material becomes much wider nowadays. In hydraulic transport in pipeline, when the suitable conveying conditions cannot be met to mobilize the particles to certain level, the solid particles in the slurry will gradually deposit at the bottom of the pipe, resulting in much higher hydraulic resistance, and potential blockage.

With the computational power nowadays, it is feasible to use the CFD method to study the solid-liquid two-phase flow in the pipeline. Among the two-phase flow models, the Eulerian-Lagrangian model can calculate the cases of various of concentrations, the Euler-Euler model has some difficulty in accurately calculating the discrete phase particles, while the ASM model [3] is only suitable for the cases of low Stokes numbers. In the Lagrangian method, DEM is know to be able to accurately describe the motion of the particle and its interaction with the fluid by considering the particle shape, the material properties, the particle size distribution (PSD) and other factors [4-6]. It can also capture the movement characteristics of coarse particles in the pipe. Liu Gang et al [7] conducted experiments and CFD-DEM coupling method to study the two-phase flow of refined oil and impurity particles in the pipeline. They analyzed the parameters such as the fluid velocity field, the pipe inclination angle and the diameter, and the impurity shape which may cause changes in the deposition patterns of the impurity particles. Chen et al [8] predicted the erosion wear rate, turbulence intensity and secondary flow velocity vector of the fluid-solid two-phase flow in 45°, 60° and 90° elbows of the pipeline, based on the

[1] Section Offshore and Dredging Engineering, Delft University of Technology, Mekelweg 2, Delft, Netherlands, X.Chen-1@tudelft.nl

[2] Associate Professor，Wuhan University of Technology，430063，Wuhan, China, bearmos@163.com

[3] Master student，Wuhan University of Technology，430063，Wuhan, China, 1227822082@qq.com

[4] Section Offshore and Dredging Engineering, Delft University of Technology, Mekelweg 2, Delft, Netherlands, S.A.Miedema@tudelft.nl

numerical simulation of CFD-DEM coupling, and it was concluded by comparative analysis that the 90° elbow is the most corrosion impact angle. Based on the CFD-DEM coupling, Zhou [9] studied the fluid mode, eddy current quantity and pressure drop of three kinds of swirl generators. It was found that the internal spiral structure is the best design for the rotary pneumatic conveying system. Though many researches have been done, there is lack for researches on two-phase pipe flow with coarse particles, where the transitions of flow regimes and concentration profiles are clearly discussed. Therefore in this project, CFD-DEM method is used to numerically study the flow patterns of slurry containing coarse particles at different line speeds. The concentration profile and the velocity field are also visited. At the end it provides a theoretical basis for the safe operation of the pipeline system in dredging practices.

2. Theoretical basis and modeling methodology

CFD is utilized for the continuum phase where the continuity and momentum equations are applied to a particle-free domain.

$$\frac{\partial \rho}{\partial t}+\frac{\partial}{\partial x_{\mathrm{i}}}\left(\rho u_{\mathrm{i}}\right)=0 \tag{1}$$

$$\frac{\partial}{\partial t}\left(\rho u_{\mathrm{i}}\right)+\frac{\partial}{\partial x_{\mathrm{j}}}\left(\rho u_{\mathrm{i}} u_{\mathrm{j}}\right)=-\frac{\partial p}{\partial x_{\mathrm{i}}}+\frac{\partial \tau_{\mathrm{ij}}}{\partial x_{\mathrm{j}}}+F_{\mathrm{i}} \tag{2}$$

where ρ is the fluid density, u_i, u_j are the fluid velocities (i, j = 1, 2, 3), P is the fluid pressure, g is the gravitational acceleration, τ_{ij} is the stress tensor and F_i is the source term representing the body force. The standard k-ε model is used to describe the turbulence. The transport equation of the model is:

$$\frac{\partial\left(\rho k\right)}{\partial t}+\frac{\partial\left(\rho k u_{\mathrm{i}}\right)}{\partial x_{\mathrm{i}}}=\frac{\partial}{\partial x_{\mathrm{j}}}\left[\left(\mu+\frac{\mu_{\mathrm{t}}}{\sigma_{\mathrm{k}}}\right)\frac{\partial k}{\partial x_{\mathrm{j}}}\right]+G_{\mathrm{K}}+G_{\mathrm{b}}-\rho\varepsilon-Y_{\mathrm{M}}+S_{\mathrm{k}} \tag{3}$$

$$\frac{\partial\left(\rho g\right)}{\partial t}+\frac{\partial\left(\rho\varepsilon u_{\mathrm{i}}\right)}{\partial x_{\mathrm{i}}}=\frac{\partial}{\partial x_{\mathrm{j}}}\left[\left(\mu+\frac{\mu_{\mathrm{t}}}{\sigma_{\varepsilon}}\right)\frac{\partial \varepsilon}{\partial x_{\mathrm{j}}}\right]+C_{1\varepsilon}\frac{\varepsilon}{k}\left(G_{\mathrm{K}}+C_{3\varepsilon}G_{\mathrm{b}}\right)-C_{2\varepsilon}\rho\frac{\varepsilon^{2}}{k}+S_{\mathrm{k}} \tag{4}$$

In the formula above, G_k is the turbulent kinetic energy due to the average velocity gradient; G_b is the turbulent kinetic energy due to buoyancy; Y_M is the effect of the compressible turbulent pulsatile expansion on the total dissipation rate; $C_{1\varepsilon}$、$C_{2\varepsilon}$、$C_{3\varepsilon}$ are the empirical constants.

The momentum equation considers the interaction with the dis-continuum phase in the following way:

$$\frac{\partial}{\partial t}\left(\rho\xi u_{\mathrm{i}}\right)+\frac{\partial}{\partial}\left(\rho\xi u_{\mathrm{i}} u_{\mathrm{j}}\right)=-\xi\frac{\partial p}{\partial x_{\mathrm{i}}}+\frac{\partial\left(\xi\tau_{\mathrm{ij}}\right)}{\partial x_{\mathrm{j}}}+n_{p}\left(F_{\mathrm{drag}}+F_{\mathrm{saffman}}+F_{\mathrm{Magnus}}\right)+\xi\rho g \tag{5}$$

Where ξ is the fluid volume fraction, n_p is the number of particles per unit volume, F_{drag}, $F_{saffman}$ and F_{Magnus} are respectively the drag force applied to each particle, the Saffman lift force and the Magnuss lift force. In Eq. (5), $n_p\left(F_{drag}+F_{saffman}+F_{Magnus}\right)$ is the interaction force between the fluid and the unit volume of particles given by a series of empirical formulas in each calculation unit [10-11].

For the dis-continuum phase, DEM is used to create and describe the movement of particles in the three dimensional domain. The Eulerian averaging is applied because the turbulent diffusion on the particles and the slip of the time-averaging velocity cannot be neglected considering the difference of the initial phase momentum.

Each individual particle is calculated by using a softball model and the model is described by Newton's equations for translational and rotational motions as follows [12]:

$$m_{\mathrm{p}} \frac{dv_{\mathrm{p}}}{dt} = F_{\mathrm{P\text{-}W}} + F_{\mathrm{P\text{-}P}} + F_{\mathrm{drag}} + F_{\mathrm{saffman}} + F_{\mathrm{Magnus}} + m_{\mathrm{p}} g \quad (6)$$

$$I_{\mathrm{p}} \frac{d\omega_{\mathrm{p}}}{dt} = m_{\mathrm{p}} \quad (7)$$

Where m_p, v_p, I_p and ω_p are the particle mass, translational velocity, moment of inertia and rotational speed respectively, F_{p-w} and F_{p-p} are the contact forces between particles and the wall and other particles, g is the gravitational acceleration, and M_p is the net torque due to the contact force.

3. Set-up of the numerical simulations

The model uses a horizontal pipe with an inner diameter D = 15.24cm and a length L of 7.5m, the internal volume of the pipeline is meshed by 646,720 CFD fluid cells. In this study, the line speed of in the pipeline are set as 2m/s, 5m/s and 8m/s, the turbulence intensity I is 5%, the particle size D is 10mm, and the input volume concentration is chosen to be 10%. The outlet pressure of the pipe is set to be the atmospheric pressure. The turbulent intensity of the reflux is 0.1%, and the volume fraction of the sand reflux is zero. An enhanced wall function is utilized for the inner wall. The Di-Felice drag model is used to apply the drag force on the particles. The lift models used are the Saffman Lift, the Magnus Lift, and the Fluid-induced torque. Table 1 shows the values of the parameters in the numerical simulation.

Table 1: Parameters used in the numerical simulation

Phase	Object	Parameter	Value
CFD	Fluid/water	Density [kg·m^{-3}]	1000
		Viscosity [kg·m^{-1}·s^{-1}]	0.001003
	Velocity-inlet	Velocity [m·s^{-1}]	2, 5, 8
	Turbulence	Turbulent intensity	5%
		Turbulent viscosity ratio	10
	Wall	Wall motion	Stationary wall
		Roughness height [mm]	0
		Roughness constant	0.5
DEM	Particles	Poisson's ratio	0.5
		Shear modulus [MPa]	10
		Density [kg·m^{-3}]	2650
		Particle radius [mm]	5
	Wall	Poisson's ratio	0.25
		Shear modulus [GPa]	10
		Density [kg·m^{-3}]	7800
	Particle-particle	Coefficient of restitution	0.05
		Coefficient of static friction	0.57
		Coefficient of rolling friction	0.5
		Interaction contact model	Hertz-Mindlin (no slip)
	Particle-wall	Coefficient of restitution	0.05

Coefficient of static friction	0.36
Coefficient of rolling friction	0.5
Interaction contact model	Hertz-Mindlin (no slip)

4. Verification study on the volumetric concentration profile

Verification study is carried out to examine the volumetric concentration profile calculated from the numerical modeling in the pipe against the measured results of Vlasak [13]. Test case is set up as described by Vlasak [13], a 4m long pipeline with a diameter of 10cm, transporting coarse particles with the particle diameter of 11mm, at a line speed of 4.1m/s. Fig. 1 shows the comparison of the concentration profiles along the vertical axis in the cross section of the pipe, where *Y* is the coordinates on the vertical axis, *D* is the pipe diameter. The experimental result was extracted when the mixture flow was in the steady state. The simulation results were extracted at the time of 5s and 10s, when the flow is also in the steady state. It can be found that in all the results, the solids concentrate in the lower part of the pipe, and the concentration is approximately linearly distributed in the numerical value, while the concentration at the upper layer of the pipe is substantially zero. The errors are within the allowable range. Therefore, the simulation method can be considered to give accurate prediction.

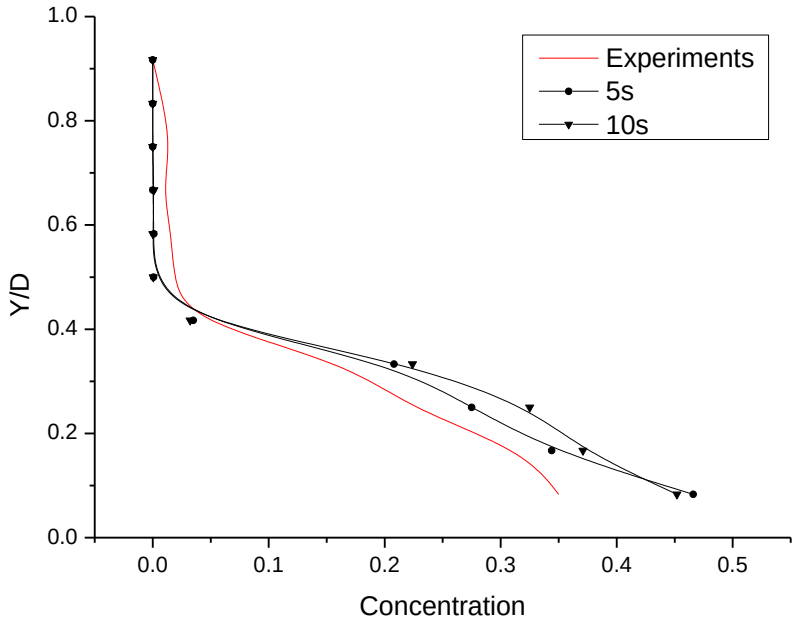

Fig.1 The comparison of experimental data with CFD-DEM simulation data on the Vlasak [13] case

5. Results and Analysis

5.1 Identification of the three flow regimes

Five flow regimes can be concluded for slurry transport [14]. In this study, three flow regimes, i.e., the fixed bed flow regime, the sliding bed regime and the sliding flow, in coarse particle transport are observed.

Fig. 2(a) shows the situation of the fixed bed flow regime captured from the simulation. The fixed bed flow is also called the restricted flow state of the pipe. In this state, the solid particles are deposited at the bottom of

the pipe, forming a bed layer of stationary particles, and the fluid can only flow through the confined space above the bed. When the accumulated particles reach a certain level, the fluid will not be able to pass through the pipe section on time, so the blockage occurs.

Fig. 2(b) shows the situation of the sliding bed flow regime captured from the simulation. The sliding bed flow is also called the sliding friction-dominated flow state. Under the action of the fluid, the particles continuously move forward at the bottom of the pipe. The erosion state is similar with that of the fixed bed flow.

Fig. 2(c) shows the situation of the sliding flow regime captured from the simulation. The sliding flow is also called the collision-dominated flow state, where the particles and particles, the particles and the pipe wall interact by collision, the particles are unevenly distributed in the cross section of the pipe, and the concentration is relatively high at the bottom.

As the line speed increases, flow regimes transfer from the fixed bed regime to the sliding bed flow, further to the sliding flow regime. It is observed that erosion happens to the fixed bed, when the speed reaches the Limit Deposit Velocity (LDV), the particles will be suspended or moved forward by the carrier fluid.

It can be seen from the above description that the LDV is the key criterion for particle flow transition. It can be calculated from the empirical formula[14] that the critical velocity of the slurry flow from the fixed bed to the sliding bed is 1.9m/s, and the critical speed from the sliding bed to the sliding flow is 3.6m/s. The change of the flow state of the slurry is not a transient phenomenon, but a process. When the critical speed is reached, a state transition does not occur immediately.

Fig. 2 (a) fixed bed flow

Fig. 2 (b) sliding bed flow

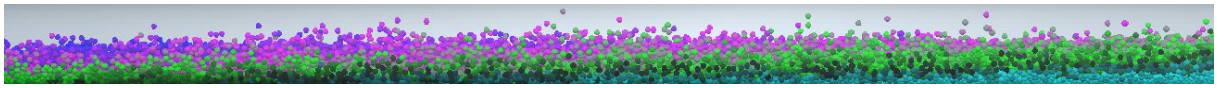

Fig. 2 (c) sliding flow

Therefore, in this study, the speeds of 2m/s and 5m/s, although higher than the critical speeds from the empirical equations, are selected to study the transition process of the flow regimes, and the higher transport speeds 8m/s is tested to study the slurry characteristics in the sliding flow regime.

5.2 Profile of the volumetric concentration of the solids

The volumetric concentration is a key parameter to identify the flow regime and predict the blockage in pipeline transport. Its profiles change with the line speed. As shown in Fig. 3, when the conveying speed is 2m/s, the particles injected from the inlet quickly settle, and the stationary portion gradually develops to a blockage which happens at the location near X = 0.5m. In the fixed bed flow, the blocked pipe section are entirely filled by particles, while behind the plugging section, only a small number of particles are at the bottom, the concentration in other spaces is almost zero.

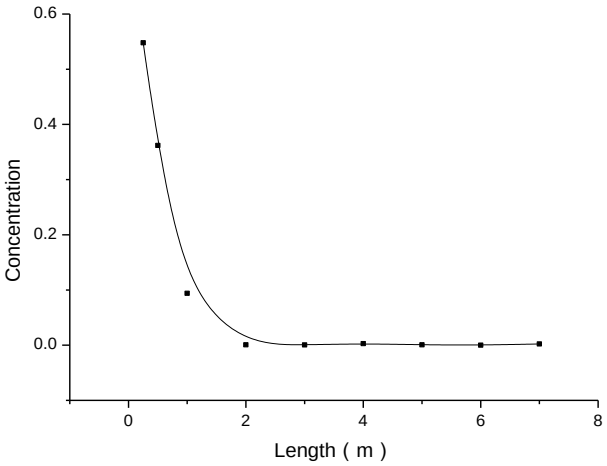

Fig. 3 Solids concentrations at different cross-sections along the pipe when the line speed is 2m/s (fixed bed flow regime)

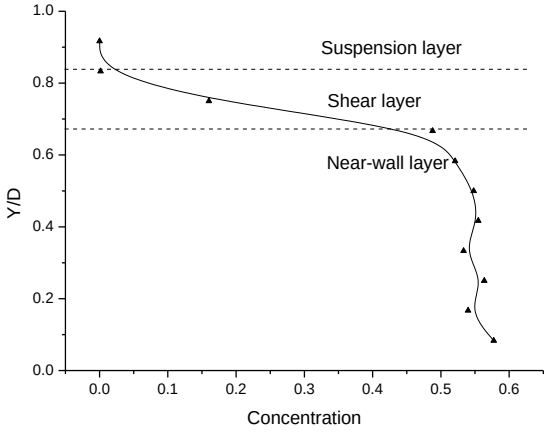

Fig.4 Concentration Profile in the cross-section at X = 4m with line speed of 5m/s (Sliding bed flow regime)

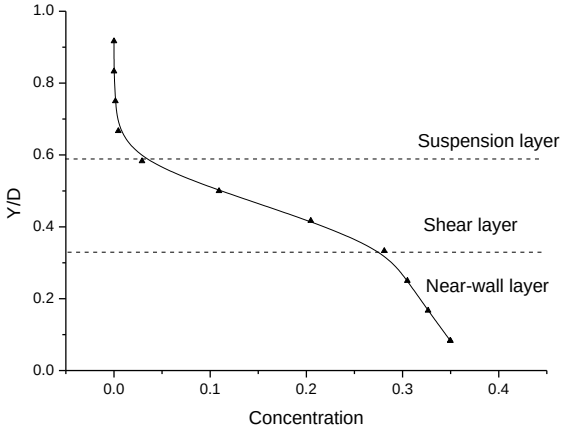

Fig. 5 Concentration Profile in the cross-section at X = 4m with line speed of 8m/s (sliding flow regime)

As the conveying line speed increases, the flow regime changes from the fixed bed flow to a sliding bed flow, and the concentration distribution also changes significantly. Fig. 4 and Fig. 5 respectively show the concentration profile in the cross section at X = 4m at the time of fully-developed flow. Both flow regimes show a lower concentration in the upper part and a higher concentration in the lower part in the pipe. The concentration distribution pattern of the sliding bed flow and sliding flow can be explained by a three-layer model.

1) The uppermost layer is the suspension layer where the particles are in suspension due to the turbulent diffusion. This layer is negligible in the sliding bed flow regime due to the fact that the coarse particles can hardly be suspended in this regime, while in the sliding flow regime there are a few particles in this layer. Due to the large flow velocity in the sliding flow regime, the shear force between the suspension layer and the shear layer is strong, so that the water can carry more particles. Therefore, the thickness of the suspension layer of the sliding bed flow is less than that of the sliding flow.
2) The middle layer is a shear layer where the particles are constantly in collisions. The motion state is maintained by the discrete forces formed by the shear stresses between the particles, and the

concentration profile is approximately linear. Due to the difference in the conveying line speeds of these two flow regimes, the carrier capacities of the fluid are also different. The shear layer thickness of the sliding bed flow regime is thinner than that of the sliding flow regime.

3) The lowermost layer is the near-wall layer where particles are transported forward as a whole. For the particles of the sliding bed flow (V = 5m/s), the concentration values in that layer remain uniform, large, and mainly at about 55%. In the sliding flow regime (V = 8m/s), the peeling action of the shear layer causes smaller thickness than that of the sliding bed, and there is certain gradient in the concentration profile.

Fig. 6 shows the variation of the solids concentration along the axial direction of the pipe. When the conveying line speed is 5m/s and the particles are in the sliding bed flow, the solids concentration fluctuates heavily along the pipe. In this kind of flow state, the particles do not uniformly distribute along the axial direction of the pipeline, but regularly disperse and aggregate to form a group, which is called a dune flow.

When the line speed is 8m/s and the particles are in the regime of the sliding flow (Fig. 7), the concentration of the solid particles will not obviously fluctuate in the axial direction after a certain distance but basically maintains at about 14%. And the particles are in the stable motion state.

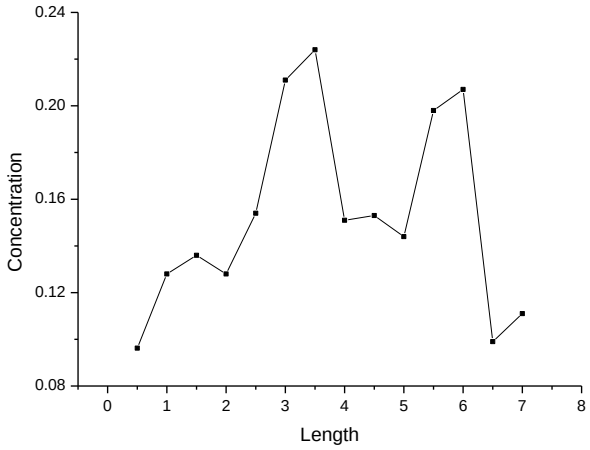

Fig. 6. Solids concentrations at different cross-sections along the pipe when the line speed is 5m/s (sliding bed regime)

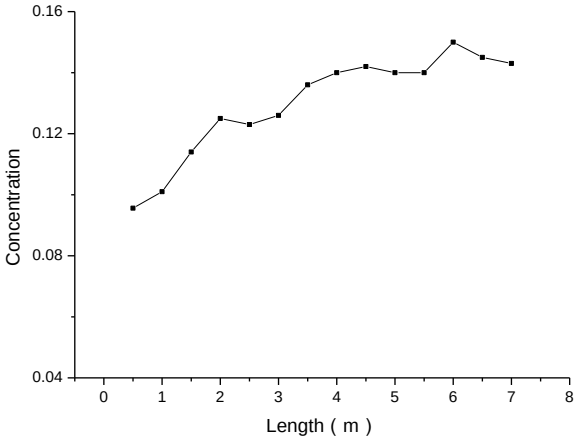

Fig. 7. Solids concentrations at different cross-sections along the pipe when the line speed is 8m/s (sliding flow regime)

5.3 Velocity field of the particles

The velocities of the DEM particles are tracked and recorded during the whole simulations, which provides with another valuable perspective for understanding the two-phase flow behavior. As shown in Fig. 8, average particle velocities at different locations along the pipeline are recorded and plotted out. When the initial velocity of the particles is 2m/s, it rapidly drops to zero at about 2m into the pipeline. After that it is hard to see any movements of the particles. The concentration distribution under the same working conditions of Fig. 3 indicates that in fixed bed flow, although the particles have a certain initial velocity at the nozzle, the solid velocity drops sharply after the entrance and blockage is gradually formed, resulting in almost no particles in the rear section of the pipeline.

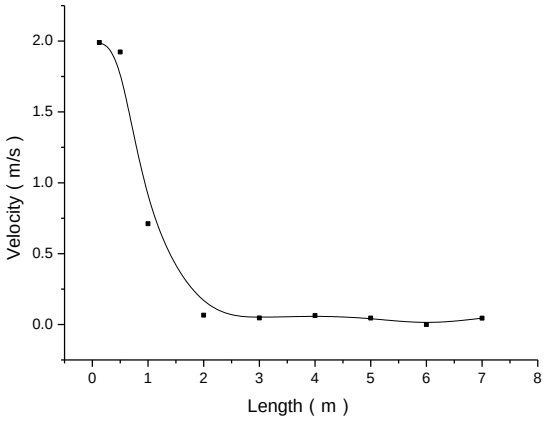

Fig.8. Average particle velocities along the pipeline, with the conveying line speed of 2 m/s (fixed bed flow regime)

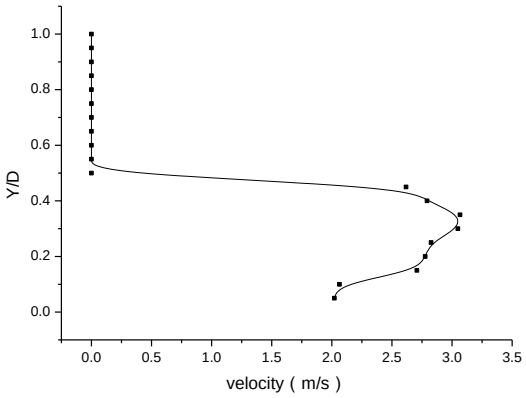

Fig. 9. Velocity profile of the particles on the cross-section when *V*=5m/s (sliding bed flow regime)

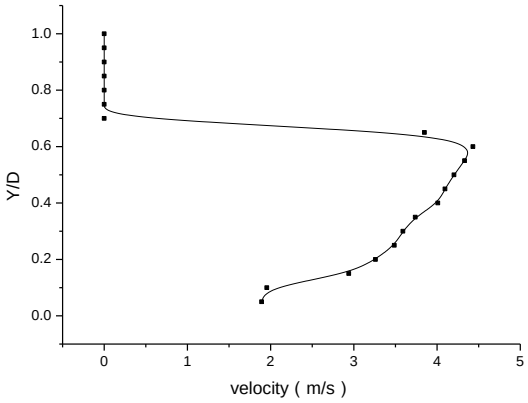

Fig. 10. Velocity profile of the particles on the cross-section when *V*=8m/s (sliding flow regime)

Fig. 9 and 10 illustrate the velocity field of the particles in the sliding bed regime (*V*=5m/s) and the sliding flow regime (*V*=8m/s). According to the velocity distribution on the cross-section of the pipeline, it is found that the maximum velocity points appear near the transition interfaces between different layers. For the sliding bed flow, it is the transition from the near wall layer to the shear layer. For the sliding flow regime, it is the transition from the shear layer to the suspension layer. It is reasonable simply because in the sliding bed flow regime, the suspension layer hardly contain any particles.

Figures 11 and 12 show the average particles' velocity at different locations along the pipe. When the particles are in the sliding bed flow regime (Fig. 11), the velocity at different sections fluctuates up and down, indicating that it is difficult to maintain a stable speed forward, and the particles exhibit a "fast-slow" pulsating motion state. When the conveying line speed reaches the level of the sliding flow regime, as shown in Fig. 12, the particles' velocities no longer change significantly with the position of the section, and the average velocity maintains at a level of about 6.5m/s after the X = 4m point. That means the mixture flow enters into the steady state after that point.

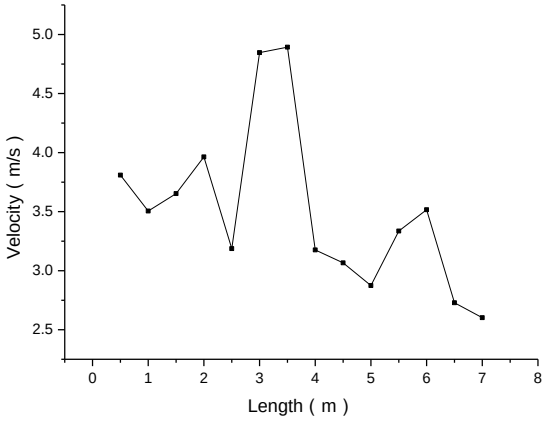

Fig. 11 Average particle velocities along the pipeline, with the conveying line speed of 5m/s. (sliding bed flow regime)

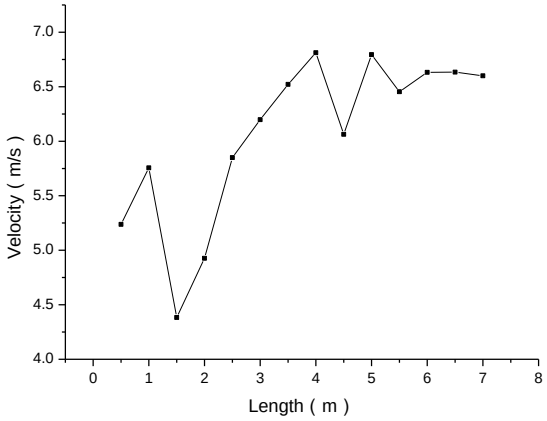

Fig.12 Average particle velocities along the pipeline, with the conveying line speed of 8m/s (the sliding flow regime)

As shown in Figure 13, in fixed bed flow regime, from the average particle velocity at the inlet of the pipe, it is found that the particle has the maximum velocity at the initial moment and then decelerates to zero in less than 2 seconds. In this flow regime, all the particles quickly become stationary near the inlet of the pipe, and gradually deposited causing the blocking accident.

In Fig. 14, under the carrying of fluid, the solid material will be settled to the bottom of the pipeline, but it does not have the ability to suspend, so it will form a “dune” in the local area due to material accumulation. The velocity of the fluid is accelerated as its passing through the narrow space above the "dune", and due to the sand-carrying effect of the fluid, the "dune" will move in the direction of flow. That is why in Fig. 14 there are apparent fluctuations on the particle velocity.

Fig. 15 illustrates the particle velocity change near the inlet of the pipe in the sliding flow regime, the particles instantaneously reach a high speed, and the peak of the maintaining speed does not change significantly with time. It is also observed at the outlet that the particles flow out of the pipeline at a constant, while slightly lower speed.

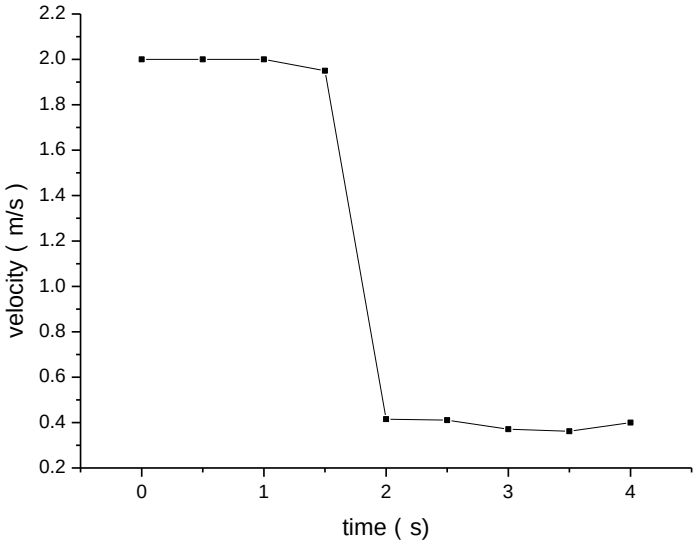

Fig. 13. Particle deceleration near the inlet of pipe when *V*=2m/s (fixed bed flow regime)

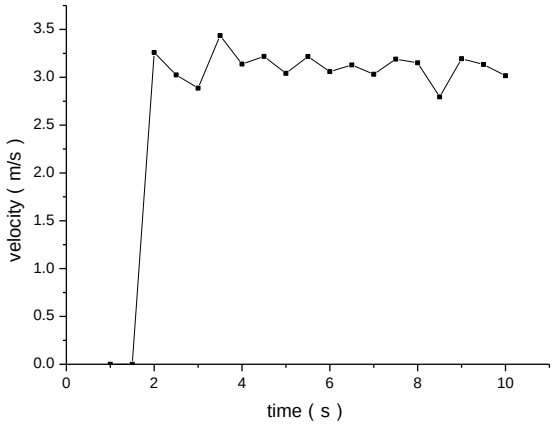

Fig. 14. Particle velocity change near the inlet of the pipe when *V*=5m/s (sliding bed flow regime)

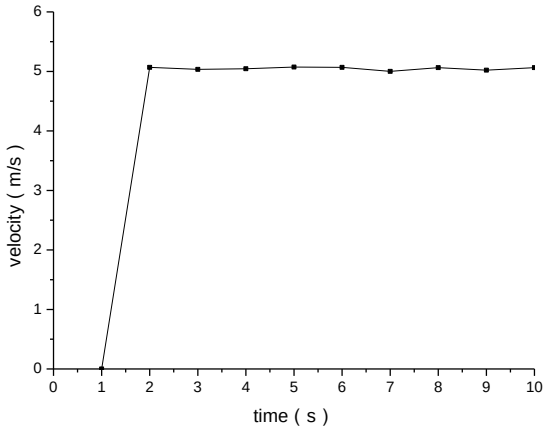

Fig. 15. Particle velocity change near the inlet of the pipe when *V*=8m/s (sliding flow regime)

6. Conclusion

In this study, the CFD-DEM coupling numerical method is used to analyze the flow characteristics and flow regime transitions of the coarse particles transported by different conveying line speeds in a horizontal pipeline. According to the analysis on the volumetric concentration distribution of the solids, and the velocity field of the particles, conclusions can be drawn are as follows:

1) The numerical modeling of CFD-DEM coupling can well simulate the dynamics of the mixture flow containing coarse particles in the pipeline. The obtained solids concentration profiles are in good agreement with the experimental data.
2) The movement patterns of the coarse particles vary with the flow regimes. In the fixed bed regime, the pipe will be blocked due to the accumulation of particles. When blockage happens, the particles fill the entire section. Only a small number of particles lay at the bottom of further locations in the pipe.
3) In the sliding bed regime, after the sliding bed reaches a certain height (about *0.55D*), the thickness of the granular bed can hardly increase much more, and then the “dune” behavior becomes significant.
4) The sliding flow regime is a relatively stable state where there are equal amounts of particles flowing in and out of the pipe. There is no apparent particle bed formation, and the concentration is non-linearly distributed in the vertical direction.
5) The velocity at different sections of the sliding flow maintains at a stable value after mixture flow is fully developed.

In summary, control on the flow regime is the key to the optimal efficiency and safety of pipeline transportation. The existence of unstable bed can lead to blockage and seriously damage the dredging operation. Therefore, in dredging practice, regionalized calibration tests are required for the coarse particles according to the local condition: the flow regime transition, and a reasonable range of the line speeds is needed to ensure that the coarse particles are transported in a steady regime of the sliding flow or heterogeneous flow in the pipeline, to achieve the energy saving goal and an efficient transportation.

Nomenclature

A_P	Pipe cross-sectional area	ρ	Density of liquid
C_{vs}	Spatial volumetric concentration	λ_r	Darcy–Weisbach friction coefficient above the particle-bed limited area
C_d	Drag coefficient	λ_l	Darcy–Weisbach friction coefficient between the liquid and the pipe wall,
C_{LM}	Magnus lift coefficient	τ_{ij}	Stress tensor
C_{LS}	Saffman lift coefficient	κ_c	Concentration eccentricity coefficient
D_p	Pipe diameter	β	Thermal expansion coefficient
d	Particle diameter	n_p	Number of particles per unit volume
D_H	Hydraulic diameter	p	Pressure
D	Deformation tensor ratio	Pr_t	Turbulent Prandtl number
F_i	Body force	R_{sd}	Relative submerged density
F_{drag}	Drag force	v_t	Particle terminal settling velocity
$F_{saffman}$	Saffman lift force	v_l	Liquid kinematic viscosity
F_{Magnus}	Magnus lift force	v_p	Translational velocity of solid phase
G_b	Turbulent kinetic energy due to buoyancy	Y_M	Effect of compressible turbulent pulsatile expansion on the total dissipation rate
G_k	Turbulent kinetic energy due to the average velocity gradient	ξ	Solid volume fraction,
κ_C	Concentration eccentricity constant	$\bar{\bar{\tau}}_s$	Stress-strain tensor of solid phase
g	Gravitational constant	e	Porosity of the particles
I_p	Moment of inertia	μ_{sf}	Sliding friction coefficient
M_t	Turbulent Mach number	ω_p	Rotational speed
M_p	Net torque due to the contact force	σ_k	Prandtl numbers corresponding to the turbulent kinetic energy
m_p	Particle mass	σ_ε	Prandtl numbers corresponding to the turbulent dissipation rate
		ε	Dissipation rate

Reference

[1] JIA Xiaomeng，LI Yongye，SUN Xihuan，et al. Research on hydraulic characteristics of pipe-conveying vehicle of charged bucket under different flow conditions[J] .Yangtze River，2017，48（14）：65-68

[2] Ni Jinren，Wang Guangqian，Zhang Hongwu. Basic theory of solid-liquid two-phase flow [M].Beijing: Science Press，1991

[3] MESSA G V, MALIN M, MALAVASI S. Numerical Prediction of Fully Suspended Slurry Flow in Horizontal Pipes[J]. Powder Technology, 2014, 256:61-70.

[4] Zhang Ke. CFD_DEM simulation of complex dense gas_solid flow [D].Hangzhou，Zhejiang University，2012

[5] Zhang Qiangqiang. Simulation Analysis of Sinking Process of Particles Falling into Water Based on Coupled DEM — CFD [D].Changchun，Jilin University，2014

[6] Yu Liming,Zou Xiaoyan，Tan Hong. 3D Numerical Simulation of Water and Sediment Flow in Hydrocyclone Based on Coupled CFD_DEM [J].Transactions of the Chinese Society for Agricultural Machinery，2016，1(1)：126-132

[7] Liu Gang, Tang Yuannan, Li Bo, et al. Movement, deposition and influence laws of impurities in the product oil pipelines[J].Oil & Gas Storage and Transportation，2017，36（6）708-715

[8] CHEN J，WANG Y，LI X，et al. Erosion prediction of liquid-particle two-phase flow in pipeline elbows via CFD-DEM coupling method[J]. Powder Technology, 2015, 275:182-187.

[9] Jia-wei Zhou, Chang-long Du, Song-yong Liu, et al. Comparison of three types of swirling generators in coarse particle pneumatic conveying using CFD-DEM simulation [J].Powder Technology, 2016, 301:1309-1320.

[10] T.Tsuji, K.Yabumoto, T.Tanaka. Spontaneous structures in three-dimensional bubbling gas-fluidized bed by parallel DEM-CFD coupling simulation. Powder Technol. 2008，184：132–140.

[11] H. Karimi, A.M. Dehkordi. Prediction of equilibrium mixing state in binary particle spouted beds effects of solids density and diameter differences, gas velocity, and bed aspect ratio. Powder Technol，2015，26：1371–1382.

[12] K.W.Chu, B.Wang, D.L.Xu, et al. CFD-DEM simulation of the gas-solid flow in a cyclone separator. Chem. Eng. Sci. 2011，66：834–847.

[13] Vlasak, P., Chara, Z., Krupicka, J., & Konfrst, J. Experimental investigation of coarse particles water mixture flow in horizontal and inclined pipes. Journal of Hydrology & Hydromechanics, 2014,62(3), 241-247.

[14] Miedema, S. A., and R. C. Ramsdell. "Slurry Transport: Fundamentals, a historical overview and the Delft Head Loss & Limit Deposit Velocity Framework." (2016).